National Défense
Defence nationale

UNCLASSIFIED
UNLIMITED DISTRIBUTION

DREV REPORT 4343/84
FILE: 3621B-005
NOVEMBER 1984

CRDV RAPPORT 4343/84
DOSSIER: 3621B-005
NOVEMBRE 1984

ON THE INVERSION OF THE LIDAR EQUATION

B.T.N. Evans

Centre de Recherches pour la Défense
Defence Research Establishment
Valcartier Québec

BUREAU - RECHERCHE ET DÉVELOPPEMENT
MINISTÈRE DE LA DÉFENSE NATIONALE
CANADA

RESEARCH AND DEVELOPMENT BRANCH
DEPARTMENT OF NATIONAL DEFENCE
CANADA

NON CLASSIFIÉ
DIFFUSION ILLIMITÉE

Canada

DREV R-4343/84 UNCLASSIFIED CRDV R-4343/84
FILE: 3621B-005 DOSSIER: 3621B-005

ON THE INVERSION OF THE LIDAR EQUATION

by

B.T.N. Evans

CENTRE DE RECHERCHES POUR LA DÉFENSE

DEFENCE RESEARCH ESTABLISHMENT

VALCARTIER

Tel: (418) 844-4271

Québec, Canada November/novembre 1984

NON CLASSIFIE

ABSTRACT

A modified form of the Klett inversion method of the lidar equation is developed. The accuracy of this inversion method is explored and validated. Unlike previous inversions, this one does not require making a guess for each lidar return to initiate the calculation.

Included are discussions of the other inversion methods. The assumptions contained in the single-scatter lidar equation and in the inversion method are outlined as is their relative importance. Special attention is given to the backscatter versus total extinction relation, multi-scattering and non-ideal detector response.

RÉSUMÉ

On a modifié la méthode d'inversion développée par Klett pour l'équation lidar. La validité et l'exactitude de cette nouvelle méthode sont démontrées. Contrairement aux méthodes déjà connues, la modification permet d'éviter l'emploi d'une estimation pour déterminer l'extinction à chaque retour du rayonnement lidar.

On discute aussi des autres méthodes d'inversion. On souligne l'importance des hypothèses dans le développement de l'équation lidar pour la diffusion unique et la méthode d'inversion. On accorde une attention spéciale à la relation entre la rétrodiffusion et l'extinction totale, à la diffusion multiple et à la réponse inadéquate des détecteurs.

TABLE OF CONTENTS

ABSTRACT/RÉSUMÉ 1

NOMENCLATURE v

1.0 INTRODUCTION 1

2.0 THE LIDAR EQUATION 2

3.0 INVERSION OF THE LIDAR EQUATION 4

3.1 Slope and Ratio Method 5
3.2 Exact Forward Inversion Method 6
3.3 Exact Backward Inversion Method (Klett's Method) 7
3.4 New Approach (AGILE) 8

4.0 VALIDATION OF AGILE 13

4.1 Remaining Problems 14
4.2 Transmission Comparisons 17
4.3 Concentration 19
4.4 Cloud Extent 22
4.5 Clear Air Extinction 22
4.6 Invariance of Inversion Point 22

5.0 QUALITY OF ASSUMPTIONS 23

5.1 Amplifier Response 23
5.2 Multi-Scattering 24
5.3 Particle Size Distribution 27

6.0 SUMMARY AND CONCLUSIONS 29

7.0 ACKNOWLEDGEMENTS 30

8.0 REFERENCES 31

FIGURES 1 to 11

TABLE I

APPENDIX A - The Effects of Clear Air Calibration 35

APPENDIX B - Correction for the Logarithmic Amplifier Response 38

APPENDIX C - Numerical and Digitization Errors 39

APPENDIX D - FORTRAN Program Listing of AGILE 43

NOMENCLATURE

A	Receiver area
B_ν	Planck emission function at frequency ν
C(r)	Clear air backscattered power at distance r
c	Speed of light
c	As a subscript refers to clear air
D	Offset distance used in calculating digitization and numerical errors
d	Constant of proportionality relating backscatter and extinction
F(r)	System function including system sensitivity and geometric crossover as a function of distance r
H	Relative change between clear air signal and peak of signal
I_ν	Specific intensity of radiation of frequency ν
J_ν	Source intensity at frequency ν
κ	Power law coefficient relating backscatter and extinction
L	Incremental distance through an aerosol
m	As a subscript refers to distance at which a guess is made
P(r)	Lidar backscattered power return at distance r

o	As a subscript refers to initial distance
$p(\mu)$	Phase function as a function of the cosine of the scattering angle μ
r	Distance or range from the lidar
S(r)	Logarithmic range-adjusted power at range r
S_E	Experimentally determined S(r)
S_T	Theoretically determined S(r)
T	Transmission
T_{inv}	Transmission as calculated by the inversion
W	Concentration
z	Parameter for adjusting correction to logarithmic amplifier and multi-scattering
α	Mass extinction coefficient
$\beta(r)$	Backscatter extinction coefficient at range r
$\sigma(r)$	Volume extinction coefficient at range r
τ	Laser pulse duration
μ	Cosine of scattering angle
ν	Frequency

1.0 INTRODUCTION

The lidar equation is the governing relation which permits the calculation of extinction and estimates of concentration under conditions of single scattering from a given lidar return. However, to obtain the solution, an inversion of the equation must be performed.

Until recently, the inversion of lidar returns to obtain extinction coefficients or concentration profiles has been plagued by instability and inaccuracies (Ref. 1). The instability of previous solutions is found to be caused by mathematical and not, as some have suggested, physical reasons. Inaccuracies can occur by making unnecessary assumptions to further simplify the equation. The solution proposed by Klett in 1981 (Ref. 1) goes a long way to improve this situation; however, as will be shown in this report, it is not quite ideal. In Ref. 2 Lentz describes a way to overcome some of these problems at high visibilities.

It seems that the inversion of the lidar equation (or radar equation with attenuation) has not been given the attention it deserves. Indeed, the basis of the ideas used in the recent solutions was contained in a paper by Hitschfeld and Bordan in 1954 (Ref. 3).

This report is an attempt to eliminate or significantly reduce the remaining problems while maintaining a simple algorithm. With the inversion of the lidar equation reduced to a simple, efficient algorithm, analysis from many lidar returns (e.g. from the Laser Cloud Mapper (LCM), Ref. 4) is possible in a short time. Appendix D gives a FORTRAN IV listing of the final program used in this report.

This work was performed at DREV between May 1981 and February 1983 under PCN 21B05, Aerosols.

2.0 THE LIDAR EQUATION

To derive the lidar equation, it is convenient to begin with the equation of radiative transfer (Ref. 5):

$$\frac{dI_\nu}{dr} = -\sigma(r)\,(I_\nu - J_\nu) \qquad [1]$$

where I_ν is the specific intensity of radiation of frequency ν in the r direction, $\sigma(r)$ is the total extinction coefficient and J_ν is the source term. J_ν contains contributions to the intensity from scattering or emission and can be given by

$$J_\nu = B_\nu + \int_1^1 p(\mu)\, I_\nu\, d\mu \qquad [2]$$

where B_ν is the Planck emission function, p is the phase function for scattering and μ is the cosine of the scattering angle. Note that in deriving [1] an important assumption has already been made: that the distance between the scatterers is larger than the wavelength used. If this condition holds, then the scattered radiation is incoherent and noninterfering.

For the next step in deriving the lidar equation, the assumption is made that $I_\nu >> J_\nu$. This assumes that no significant amount of emission or scattering from the medium are placed in the direction of propagation. Note that this contains the critical assumption that only single scattering events occur. In making this assumption we obtain

$$\frac{1}{I_\nu}\,\frac{dI_\nu}{dr} = -\sigma(r) \qquad [3]$$

or

$$I_\nu = I_{o\nu} e^{-\int_o^r \sigma(r')dr'} \qquad [4]$$

with $I_{o\nu}$ being the initial intensity of the beam before any extinction. Equation 4 is of course the well-known Beer's law.

For light that is being received in the direction opposite to the beam direction, the intensity received will be proportional to $I_{o\nu}$, geometric attenuation $\frac{A}{r^2}$, where A is the receiver area, and the folded laser pulse length given by $\frac{c\tau}{2}$, where c is speed of light and τ is the time duration of the laser pulse. Furthermore, the intensity will depend on the probability of being backscattered at a range r, $[\beta(r) = p(-1)]$, and finally a system function F(r) which includes factors such as system sensitivity and geometric crossover of the receiver and laser beam. Putting all these factors together with [4] and noting the power received $P(r) \propto I_\nu(r)$, we obtain the lidar equation:

$$P(r) = P_o \frac{c\tau}{2} \frac{F(r)\beta(r)}{r^2} A e^{-2\int_o^r \sigma(r')dr'} \qquad [5]$$

where P_o is the initial laser pulse power. Here, the extinction term in Beer's law has been squared, since the returned power must traverse the same medium twice.

In summary, the derivation of [5] has required the following assumptions:

1. incoherent scatterers (Equation of Radiative Transfer);
2. no significant emission $I_\nu >> J_\nu$;
3. first-order multiple scattering;
4. only backscatter is received, $\beta(r) = p(-1)$ [$\beta(r)$ could be properly integrated over μ];

5. only a plane wave is received, i.e. even light distribution over area A (one can use an effective area);

6. no beam pulse stretching (τ does not change);

7. receiver encompasses laser beam; beam overlap is complete and there is no blind spot ($1/r^2$);

8. invariance of the phase function over small solid angles;

9. $\sigma(r)$ is independent of P_o;

10. particles are not in the shadow of each other (particles act independently); and

11. the light source is monochromatic.

3.0 INVERSION OF THE LIDAR EQUATION

In the lidar equation [5], it is usually the term $\sigma(r)$ that is the unknown of greatest interest. It can be seen however that this equation has three unknowns: $\sigma(r)$, $\beta(r)$ and $F(r)$.

$F(r)$ is usually estimated or obtained by a calibration experiment reducing the problem to two unknowns. In order to proceed, a further assumption must be made, that is

$$\beta(r) = d\sigma^k \qquad [6]$$

Klett has made a literature search which indicates that $0.67 < k < 1.0$ (Ref. 1). Indeed, it seems that for water fogs, $k = 1$ is the value most often reported (with proportionality constant $d = 0.05\ Sr^{-1}$ (Refs. 6, 7, 8)). However, for other types of aerosols (e.g. snow, burning phosphorus clouds, silica dust, etc.), there is

less information available and furthermore, if the size distribution changes in regions involving the lidar signal, k will probably vary. For a theoretical study, see Ref. 9. More will be said on this assumption later in this report (Chapter 5.0).

With this final assumption [6], the lidar equation can now be solved for $\sigma(r)$. In order to simplify [5] the following definition is usually made:

$$S(r) = \ln[r^2 P(r)] \qquad [7]$$

Taking the derivate of S(r) with respect to range, plus the lidar equation [5] with F(r) a constant and the assumption [6], we get

$$\frac{dS}{dr} = \frac{k}{\sigma}\frac{d\sigma}{dr} - 2\sigma \qquad [8]$$

In deriving [8], both F and d disappear. This will be important in Section 3.4.

The following three sections briefly review the major inversion methods to date and a fourth section describes the development of the modified inversion method. All four sections discuss the strengths and weaknesses of the various methods.

3.1 Slope and Ratio Method

This method will only be mentioned briefly since its value as a solution has greatly diminished with the advent of the newer solutions.

If one assumes that over some distance the aerosol is uniform, we can have $\frac{d\sigma}{dr} = 0$. Therefore, from [8],

$$\sigma = -\frac{1}{2}\frac{dS}{dr} \qquad [9]$$

so that the slope of a plot of S versus r will give us the value of σ over the homogeneous region. This can be a very poor approximation if there is noise or if the cloud is inhomogeneous. In general, an aerosol that produces a positive slope in S (likely in a very inhomogeneous medium) will give negative σ by this method!

The ratio method is just a variant of the slope method when it is applied segment by segment (see Ref. 10). Note also that [9] would result from the assumption that $k = 0$, i.e. the backscatter coefficient is a constant independent of the cloud concentration. Even with the problems listed above, it is the slope method that has been used the most often in the past since it is simple and the only widely known method.

3.2 Exact Forward Inversion Method

In 1954, Hitschfeld and Bordan (Ref. 3) solved the differential equation [8] exactly. It is not difficult to solve because it is a standard differential equation, namely a homogeneous Ricatti equation. The solution is

$$\sigma(R) = \frac{\exp[(S - S_o)/k]}{(\sigma_o^{-1} - \frac{2}{k}\int_{r_o}^{r}\exp[(S - S_o)/k]dr')} \qquad [10]$$

where the subscript o refers to the reference distance r_o which is closest to the lidar system. This solution requires knowledge of σ_o which can be measured or guessed. However, as Klett emphasized (Ref. 1), this solution is unstable since two relatively large terms are subtracted in the denominator to obtain a small difference. Thus, if there is an error in σ_o, the solution quickly becomes unstable and unrealistic values of σ are computed at modestly small r. See Refs. 1

and 2 for more details on the error analysis of this solution. It is this instability that has caused the exact forward inversion method to be neglected in favor of the slope method.

3.3 Exact Backward Inversion Method (Klett's Method)

It seems surprising to find that, until 1981, no one had published the idea of making the guess or measurement of σ_o in [10] at the largest distance from the lidar system, even though this idea was mentioned in Ref. 3 and a more generalized version was discussed in Ref. 11. It appears that some unsuccessful attempts were made (Refs. 12, 13). However, using this idea, Klett obtained the following solution:

$$\sigma(r) = \frac{\exp\left[(S - S_m)/k\right]}{\left(\sigma_m^{-1} + \frac{2}{k}\int_r^{r_m} \exp\left[(S - S_m)/k\right]dr'\right)} \qquad [11]$$

where the subscript m refers to the reference distance r_m which is furthest from the lidar system. Now the two expressions are added in the denominator, making the solution more stable, and furthermore, the error in σ_m (which must be estimated for each return) becomes less important as r decreases since the integral in [11] increases. Thus the solution will tend to converge to the correct $\sigma(r)$ as r gets smaller.

Even though this solution is greatly superior to [10], some problems still remain. If, for example, we take the case of high visibility, it can be seen that the integral of [11] is very small and indeed can be considered near zero in comparison with σ_m^{-1}. If this happens we get:

$$\sigma(r) \approx \sigma_m \exp\left[(S - S_m)/k\right] \qquad [12]$$

Thus all resulting extinction coefficients become linearly related to σ_m and hence to the error in σ_m. From this, it is apparent that, in the case of high visibility, the solution [11] is not very stable.

This problem can be overcome (Ref. 2) by calibrating the lidar system to find the system constants. Indeed, the very need for making a guess (σ_m) in this solution is created by the derivation of the differential equation [8] in which the absolute constants drop out. The guess can therefore be seen as an attempt to put back this information. Thus, in obtaining the system constant, one can make a better guess. After a guess has been made, theoretically calculated values of S (S_T) can be computed from estimated extinction coefficients. These, in turn, can be compared with experimentally obtained S (S_E) (computed directly from the lidar return by $S_E = \ln(P/C)$. The procedure in Ref. 2 is to sum all S_T and match them with S_E by making

$$\Sigma(S_E - S_T) = 0 \qquad [13]$$

The summation is intended to minimize noise in the signal. This method produces an acceptable inversion for the high visibility case.

3.4 New Approach (AGILE)

A new approach called AGILE (Automatically Generated Inversion of the Lidar Equation) is developed in this section. This approach was adopted because the following problems still remain with the Klett method:

1. For the high visibility case, several iterations are needed to minimize the sum in [13]. It is also possible that this condition is not strong enough. For example, if one has a rapidly varying cloud of low density, there will be large numerical errors occurring in the summation of [13]. These

errors could make the sum zero without it necessarily being a good inversion (see the discussion of numerical errors in Appendix C).

2. For the medium visibility case, the convergence of the Klett method is still not fast enough, since perhaps half of the values of the lidar return are spent converging to the correct value. Therefore only the front half of the shot is good. A procedure of the type used in Ref. 2 could help, but will require on the average many iterations as well as the evaluation of the integral $\int_o^r \sigma(r')dr'$ with the ensuing numerical errors.

3. At low visibilities, one can expect rapid convergence by the Klett method, but now another problem arises which can make the resulting inversion poor. This is caused by the theoretical limit of the integral in [11], as will be shown below. If this limit is exceeded due to numerical or experimental errors or incorrect assumptions, the resulting inversion will give values for σ that become increasingly smaller than the true value as r decreases.

The proposed modification is an attempt to eliminate or significantly reduce the above-mentioned problems in the inversion of a lidar signal.

If we start with the lidar equation [5] and write it for the case of the clear air returned power value C(r) (as done in Ref. 14), we have

$$C(r) = P_o \frac{c\tau}{2} F(r) \frac{Ad\sigma_c^k e^{-2\sigma_c r}}{r^2} \qquad [14]$$

where σ_c is the clear air value of the extinction coefficient and we have taken σ_c constant over r. If we now divide P(r) by C(r) and rearrange, we get

$$e^{-2\sigma_c r}\,\sigma_c^k\,\frac{P(r)}{C(r)} = \sigma^k e^{-2\int_0^r \sigma(r')dr'} \qquad [15]$$

This result has assumed that the clear air aerosol and the cloud have the same value of d (which is not necessarily true but which does not affect the result). This is because we can take σ_c as an effective clear air extinction coefficient (since we are not interested here in clear air extinction). Taking the k-th root of each side of [15] and integrating over r, one obtains

$$\int_0^r \sigma_c\left[\frac{P(r'')}{C(r'')}\right]^{\frac{1}{k}} e^{-\frac{2}{k}\sigma_c(r')r''}\,dr'' = \int_o^r \sigma(r'')e^{-\frac{2}{k}\int_0^{r''}\sigma(r')dr'}\,dr''$$

$$= \frac{k}{2}\left[1-T(r)^{2/k}\right] \qquad [16]$$

where T(r) is the transmission at the distance r. To further simplify we will assume that σ_c is small enough to be negligible (i.e. $\sigma_c \ll k/2r$) to give

$$\frac{2}{k}\,\sigma_c \int_0^r \left(\frac{P}{C}\right)^{1/k} dr'' = \left[1 - T^{2/k}\right] \qquad [17]$$

where it is now understood that P, C and T depend implicitly on r. The importance of this result can be seen when it is understood in terms of its physical significance. Equation 17 states that the normalized integrated backscatter has a limit. In dividing the power return P by the reference signal C (in this case, a clear air shot), one calibrates the laser shot against system constants, system noise and against the $1/r^2$ factor. The resulting improvement of the signal is demonstrated in Appendix A.

The integral in [17] represents a sum over distance or time of the power received during one shot or of the total power received (or equivalently, the normalized integrated backscatter). Equation 17 then states that this has a maximum, i.e.

$$\frac{2}{k}\,\sigma_c \int_0^r \left(\frac{P}{C}\right)^{1/k} dr'' \to 1 \text{ as } T \to 0 \qquad [18]$$

If this limit is exceeded then there is either significant experimental error (e.g. detector downtime), numerical/digitization errors or some physical assumption is no longer valid (e.g. multi-scattering). This then provides an immediate check, albeit weak, on the system, inversion method and physical assumptions. It should be noted that limits similar to those in [18] can be derived for larger valves of r where σ_c is no longer small enough.

Another feature of [17] is that, knowing the sum of the power received at a given point, one can immediately calculate the transmission. This allows knowing T without doing the inversion to get σ (and consequently eliminates another pass through a numerical integration).

Finally, the integral in [17] is equivalent to the integral in Klett's solution [11]. In fact, writing Klett's solution [11] after calibrating with C(r), one obtains

$$\sigma = \frac{\sigma_c (P/C)^{1/k}}{\dfrac{\sigma_c (P_m/C_m)^{1/k}}{\sigma_m} + \dfrac{2}{k}\,\sigma_c \displaystyle\int_r^{r_m} \left(\frac{P}{C}\right)^{1/k} dr'} \qquad [19]$$

The lidar equation can be written as (from [15])

$$\sigma = \frac{\sigma_c\,(P/C)^{1/k}}{T^{2/k}}\,. \qquad [20]$$

By noting that

$$\frac{\sigma_c (P_m/C_m)^{1/k}}{\sigma_m} = T_m^{2/k} \qquad [21]$$

from [20], and

$$\frac{2\sigma_c}{k} \int_r^{r_m} \left(\frac{P}{C}\right)^{1/k} dr' = (T^{2/k} - T_m^{2/k}) \qquad [22]$$

a generalization of [17], it can be seen that Klett's solution is just a restatement of the lidar equation (except that σ_m or T_m are guessed).

Again substituting [17] into [20], we get the solution in a different form:

$$\sigma = \frac{(P/C)^{1/k}}{\sigma_c^{-1} - \frac{2}{k} \int_o^r \left(\frac{P}{C}\right)^{1/k} dr''} \qquad [23]$$

This is similar to the forward inversion method (Section 3.2) except that σ_o is replaced by σ_c. Or, equivalently, Klett's solution becomes

$$\sigma = \frac{(P/C)^{1/k}}{T_m^{2/k}/\sigma_c + \frac{2}{k} \int_r^{r_m} \left(\frac{P}{C}\right)^{1/k} dr'} \qquad [24]$$

Equations 23 and 24 are equivalent since they guarantee that

$$S_T(r) = S_E(r) \qquad [25]$$

at each interval of r, a condition much stronger than [13], providing that errors do not invalidate [18]. This can be seen because of [17] and [20] and the definition of S_T and S_E. This condition, [25], is

not satisfied by Klett's solution [11] because of possible errors in the guess, σ_m. With solutions [23] or [24], once a calibration shot has been made and a value of σ_c obtained, no guessing will be needed as long as the value of σ_c and the calibration remain valid. (The values of σ_c can be obtained by a trial inversion of one shot in which the transmission is measured, or by other means). This has great advantages over the other methods when many shots under the same conditions must be processed. Plus, the necessary condition [25] is automatically satisfied, whereas in the Klett method the weaker condition [13] must be converged to and may still give significant errors.

4.0 VALIDATION OF AGILE

In this chapter, evidence of the success of AGILE will be reviewed and compared with Klett's solution. The remaining difficulties will be discussed, as will an indication of the numerical and digitization errors. The lidar data used in this section was obtained from the DREV Laser Cloud Mapper (LCM) (Ref. 4), with clouds produced by burning red phosphorus.

What constitutes a good inversion of the lidar equation [5] along with the assumption [6]?

It is necessary and sufficient that a good inversion satisfy the condition [25] and uses the correct value of σ_c. Equation 13 is only a necessary condition.

Since many assumptions have been made to obtain [23] or [24], how can a check be done to indicate that the results from the inversion are a good representation of the real values? The following items will be compared and discussed in detail in this chapter in order to indicate the successes and limitations of the current inversion:

1. the transmission of this inversion with respect to that obtained from Klett's method (with the estimation procedure as outlined in Ref. 2);

2. the transmission with that obtained directly by the LCM;

3. the extinction coefficients and concentrations found typical by this method in burning red phosphorus smoke and those from in situ measurements;

4. cloud extent;

5. clear air extinction coefficients in front of and behind the cloud; and

6. the results obtained should be independent of the inversion starting points in the shot.

4.1 Remaining Problems

With this new approach, two calibration shots are needed: one in clear air (or through a uniform medium) and the other with some transmission loss in order to determine σ_c. With the LCM this is not a problem, since this system is capable of making 100 shots per second, all in different directions and many through clear air.

Once σ_c and a good clear air shot have been obtained, the biggest remaining problem results from the possible errors in the evaluation of the integral in [23] or the integral and T_m in [24]. This is caused mainly by errors arising from the system response or multi-scattering. For if the system response is too slow in recovery and/or the cloud is dense enough for multi-scattering to be present, the limit [18] could easily be surpassed. If this happens, neither [23] nor [24]

can work, and neither can the Klett solution. This occurs simply because the lidar equation has become invalid.

If, however, the system response is not too bad, a correction can be applied. Multi-scattering poses a much more serious problem and there are currently no simple or accurate corrections for this phenomenon. Therefore it is suggested that in performing an inversion using the lidar equation [5], a guarantee of the limit [18] should be given. This can be done by decreasing the return values in the individual shots as the range increases, according to how rapidly the normalized integrated backscatter (or limit [18]) is approached. Since the functional form needed for reducing the return values is not generally known, estimates must be used (which adds some uncertainty to the results). However, one needs to know this function only in the extreme case of very dense clouds and can be calibrated to some extent.

The functional form used for the multi-scattering is the same as that used to correct for the logarithmic amplifier (see Appendix B). Thus a single correction term (or the same form used by Ref. 15) with one adjustable parameter attempts to correct for multi-scattering and the amplifier response (and any other reason that may cause the limit in [18] to be exceeded). This factor is just T^{-z} with z being the adjustable parameter. Since both effects are combined, z will be larger than if only one effect were present.

With the data presented in this report, $z = 0.8$ was found to give good agreement with target reflectance. The value of this parameter in Ref. 15 is shown to be $0.2 < z < 0.3$, with pure multi-scattering, a field of view between 5 and 10 mrad and a size distribution similar to that considered in the above-mentioned data. Thus for the value of $z = 0.8$, about 30% is caused by multi-scattering. This factor is used only when the optical depth becomes less than unity.

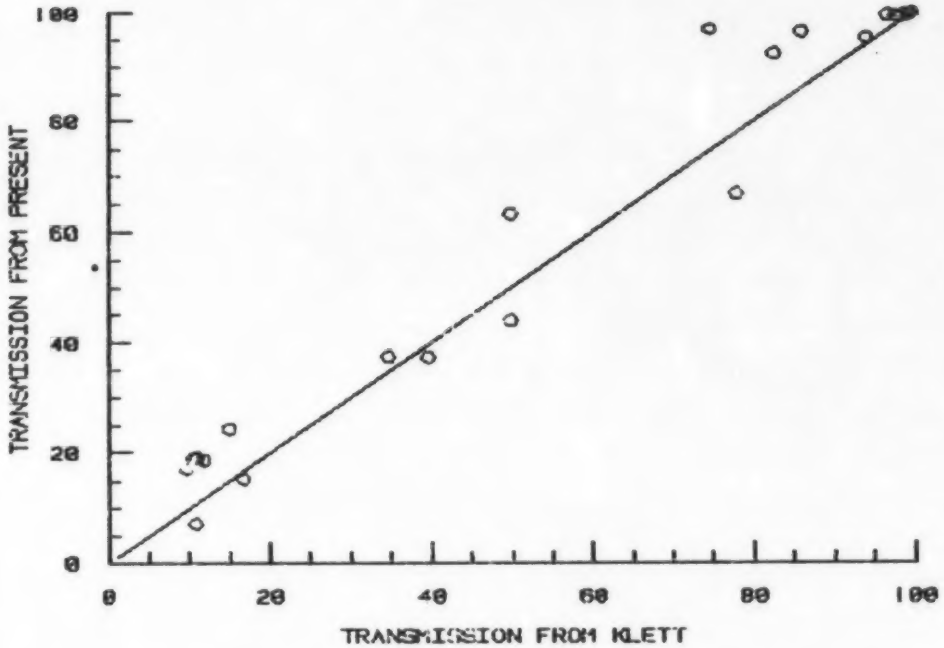

FIGURE 1 - Transmission comparison of new inversion versus Klett's solution

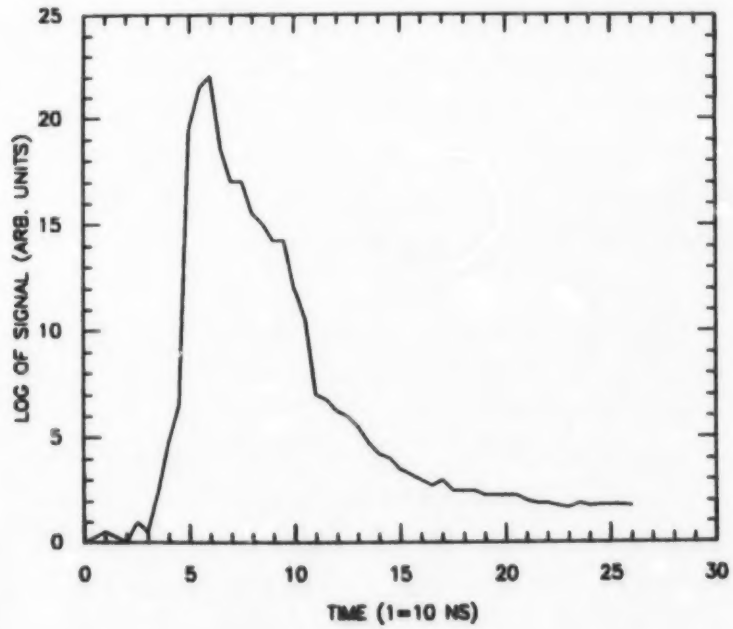

FIGURE 2 - Response of the logarithmic amplifier

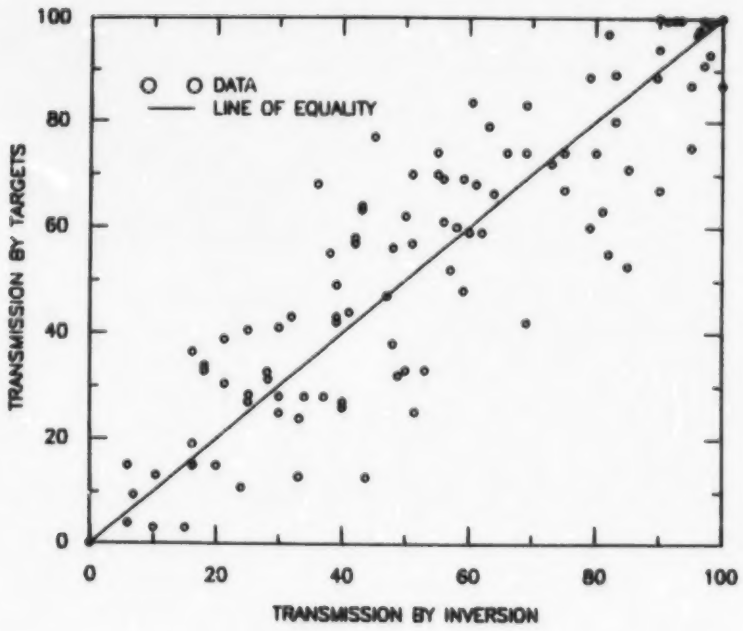

FIGURE 3 - Comparison of transmissions by inversion versus by targets

4.2 Transmission Comparisons

A comparison between the transmission computed from the present method and that computed by Klett's method (Ref. 1) is shown in Fig. 1. The graph shows that there is excellent agreement between the two methods. However, there is still some scatter. One reason for discrepancies is the difficulty in making the proper guess in the Klett method in denser clouds, especially when there is significant signal at the point in the shot where the guess is being made. This difficulty is due to numerical and digitization errors that occur when calculating the integrals and obtaining the transmission.

Another source of error is the response of the amplifier used in processing the return signal. Figure 2 shows the response of the logarithmic amplifier in the LCM. The vertical scale is the logarithmic output in arbitrary units, and the horizontal scale is the time in nanoseconds. From this, and with a digitization rate of 10 ns, one can see that the rise time of this amplifier is adequate but that the downtime will cause problems, especially when the signal is large and varies rapidly. Thus, in attempting to correct for this response (see Appendix B or Section 4.1), errors will occur in both programs since perfect correction is impossible.

Figure 3 is a plot of the transmission calculated from the new algorithm versus the transmission as measured by the intensity of the signal returned by cooperative targets. Again the agreement is reasonable but there is some discrepancy. Most of this discrepancy can be explained by the variation in target uniformity and errors in the laser firing angle. These errors account for a variation of about ± 20%.

Other errors that can cause disagreement in Fig. 3 are the problems outlined above, i.e. amplifier response, numerical and digitization errors, plus, perhaps, significant multi-scattering for transmission much less than 40% (about one optical depth). A least mean squares fit of the points gives a straight line:

$$T_{inv} = 0.91T_E + 5.18 \qquad [26]$$

with a correlation coefficient of 0.81, where T_{inv} and T_E are the transmissions obtained from inversion and experiment respectively. The correlation coefficient value seems most reasonable when the variation in the target reflectance is considered.

4.3 Concentration

As already mentioned, the data here were taken by the LCM from a red phosphorus generated smoke. By using values for the mass extinction coefficients (taken from the DREV silo and ≈ 50% relative humidity), a conversion of the total extinction coefficient into concentration is possible by the relation

$$\sigma = \alpha W \qquad [27]$$

where α is the mass extinction coefficient, W is the concentration in grams per cubic centimeter and L is the path length in centimeters. This relationship has been verified by many studies (both theoretical and experimental) over widely varying types of aerosols, densities and wavelengths (see for example Refs. 16-19). With such a calculation of concentration, a comparison between the calculated and measured concentrations can be made. Unfortunately no direct measurement of the concentration was made when these lidar data were taken, but the purpose here is to show that the concentration values obtained by the inversion are reasonable "ballpark" figures.

DREV and others (Refs. 16, 20-22) indicate $\alpha = 1.5\text{-}2.5\ m^2/g$ at 1.06 μm and 50% R.H. Furthermore, one can obtain from the literature in situ field values of the concentration for red phosphorus generated smokes (Ref. 23). Table I gives a comparison between typical variations in concentrations between the calculation in this report and in Ref. 23. The correspondence between the two indicates a satisfactory agreement. Thus the calculations done here give a good order of magnitude estimate of the actual field values during the experiment.

TABLE I

Comparison of field trial concentrations of red phosphorus smoke

	mg/m^3
Smoke Week III (Ref. 6)	5-200
Present Study	0.1-300

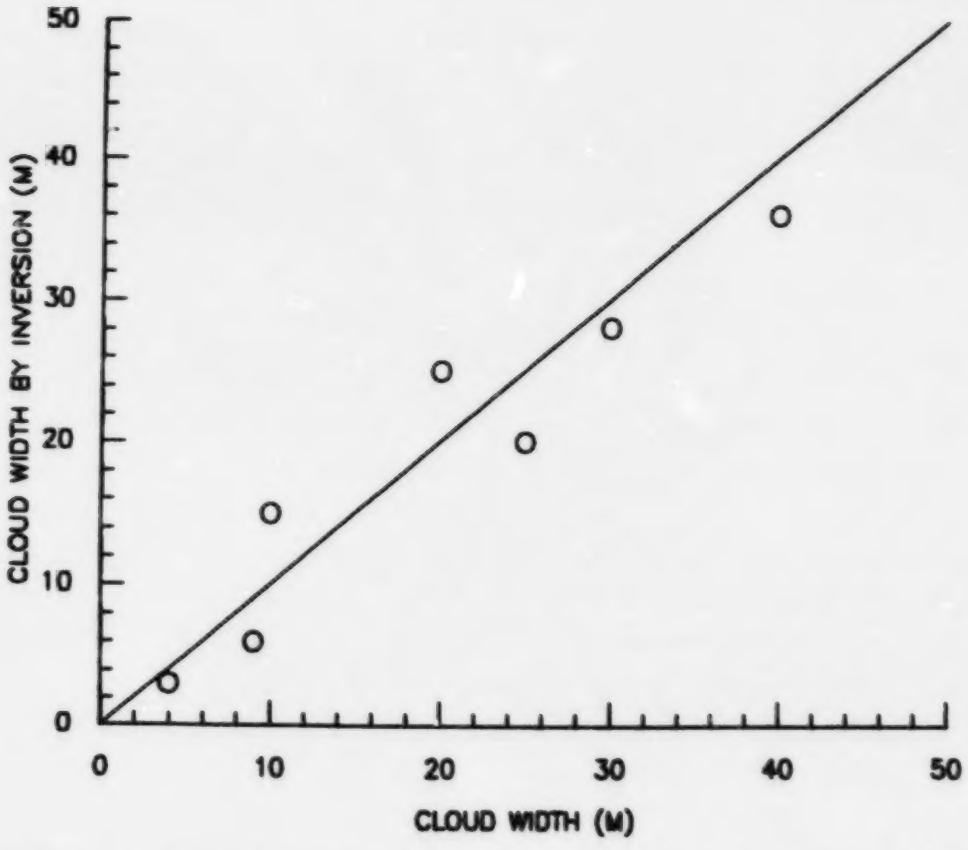

FIGURE 4 - Comparison of cloud extent calculated by inversion and by photographic measurement

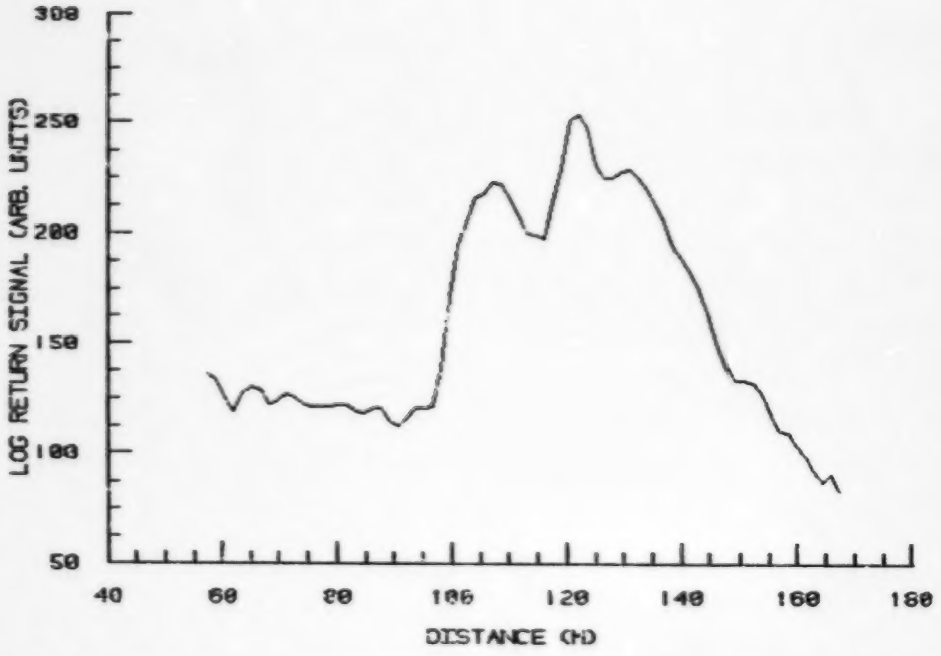

FIGURE 5 - Example of raw lidar return signal versus distance for an RP smoke

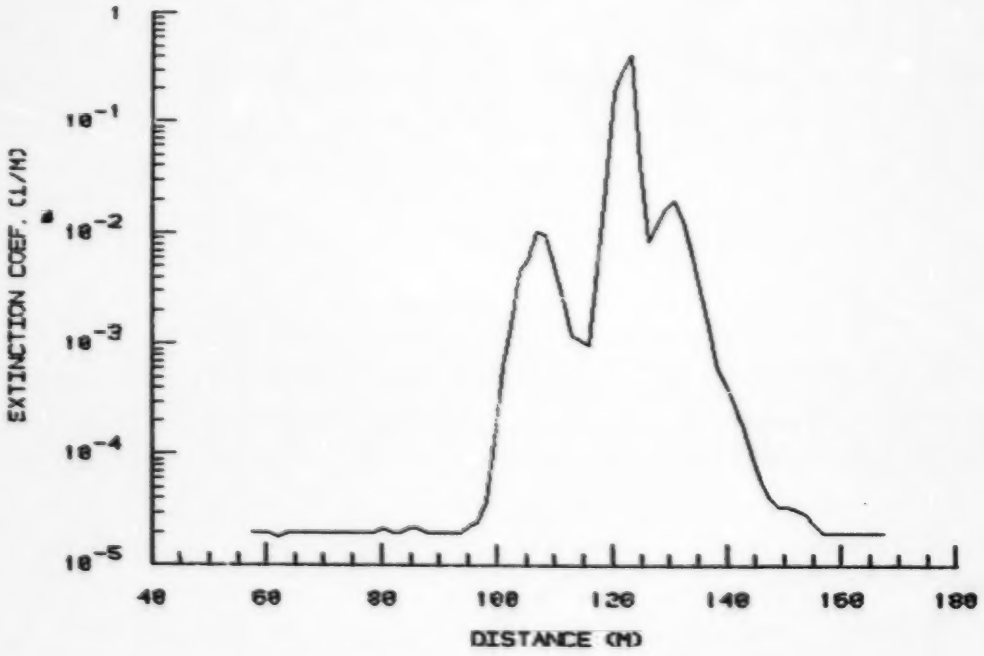

FIGURE 6 - Inversion of the raw data in Fig. 5

4.4 Cloud Extent

During the trials, photographs were taken of both the front and back of the cloud. This allows one to estimate the cloud extent photographically. Figure 4 is a plot of the calculated cloud extent along one laser line and the estimate from the photographic data. Differences can obviously occur because of the difficulty in estimating the location of the cloud edges. In the photograph, this is due to lack of contrast and in the lidar data, it is due to the definition of what is cloud and what is clear air. The agreement is good. The importance of this agreement will be discussed in the next chapter in relation to the assumptions made.

4.5 Clear Air Extinction

Figures 5 and 6 are examples of a raw lidar signal and the resulting inversion for one shot. Figure 6 shows the calculated extinction coefficient plotted against distance from the LCM (or lidar system). The important feature to notice here is that the clear air extinction values in front of and behind the cloud agree very well. This is essential and verifies the calculated transmission through the cloud.

4.6 Invariance of Inversion Point

A necessary property that all inversions should have is that the inversion should be independent of the initial starting point, i.e. overlapping results of differently initiated inversions should be identical. The new solution guarantees this because of the condition $S_E = S_T$. However for the Klett method, errors in the guessed value σ_m will in general produce values different from guesses made at other distances. Thus the resulting calculation will be different. As the cloud density increases and/or varies rapidly, this problem becomes

more important, especially for guesses made inside the cloud. This invariance is obtained because of the normalization of the lidar return by the clear air.

5.0 QUALITY OF ASSUMPTIONS

Many assumptions have been made in the derivation of [23] and [24] and their subsequent use. An attempt is made here to identify the most important assumptions and their effect on the accuracy of the inversion. Most of the assumptions leading to the lidar equation (Chapter 2.0) are excellent approximations to the conditions under which the current data were taken. Major exceptions are the assumption of single scattering (for dense clouds) and the invariance of the phase function. In this case, it is a possible variation in the size distributions of the particles. This latter assumption is also involved in the relation [6] and when $k = 1$, which is a constant with respect to r. But perhaps the most important effect is that of the logarithmic amplifier's response.

5.1 Amplifier Response

The time response of the amplifier has already been given in Fig. 2. A good check to see if the response of the amplifier is being adjusted for correctly (see Appendix B) is to pass a lidar return from a target through the inversion with this correction. Figure 7 is the result of such a calculation. Note that the program has now considerably compensated for the downtime and a relatively sharp response remains.

The target response can be considerably enhanced with a Fourier transform and deconvoluted with a Wiener filter (Ref. 24), but the results, as indicated in Fig. 8, show that the noise is considerably amplified and the absolute values become unreliable.

Figure 9 is an illustration of results obtained from a scan of an HC (hexachloroethane) smoke without compensation for the logarithmic amplifier. The disturbance in this cloud map occurs for extinction coefficients as large as 10^{-3} m^{-1}. Figure 10 shows the same cloud once the logarithmic amplifier response has been corrected. Notice that even at the lowest extinction coefficient, which is considerably smaller than any in Fig. 9, there are no distortions of the cloud contouring. The cloud maps of Figs. 9 and 10 are computer calculated and drawn and are in the form seen by the user of the program (Ref. 25). Note that similar distortions due to multi-scattering could occur in clouds.

5.2 Multi-Scattering

The various experiments and theory that have so far been considered in the literature make it very difficult to ascertain the effects of multi-scattering for a given beam geometry, field of view, lidar system distance, aerosol, wavelength, size distribution, etc. (Refs. 15, 26-28). Indeed, many of the parameters on which multi-scattering depend may only be known vaguely or not at all (e.g. particle size distribution and particle shape).

When the cloud is dense enough, significant multi-scattering will invalidate the lidar equation. Thus, either a new lidar equation incorporating multi-scattering should be used or the data adjusted so that only the single-scatter component of the signal is considered.

By examination of the available theories and experiments (e.g. Refs. 15, 26-28), a good rule of thumb would be to consider multi-scattering when the optical depth is greater than 0.1 for lidar systems approximately 1 km or more from the cloud and perhaps for optical depths greater than 1.0 when the lidar system distance is close (about 50-100 m), as is the case with the LCM. This assumes that the field of view of the lidar system is roughly in the range of 1 to 10 mrad.

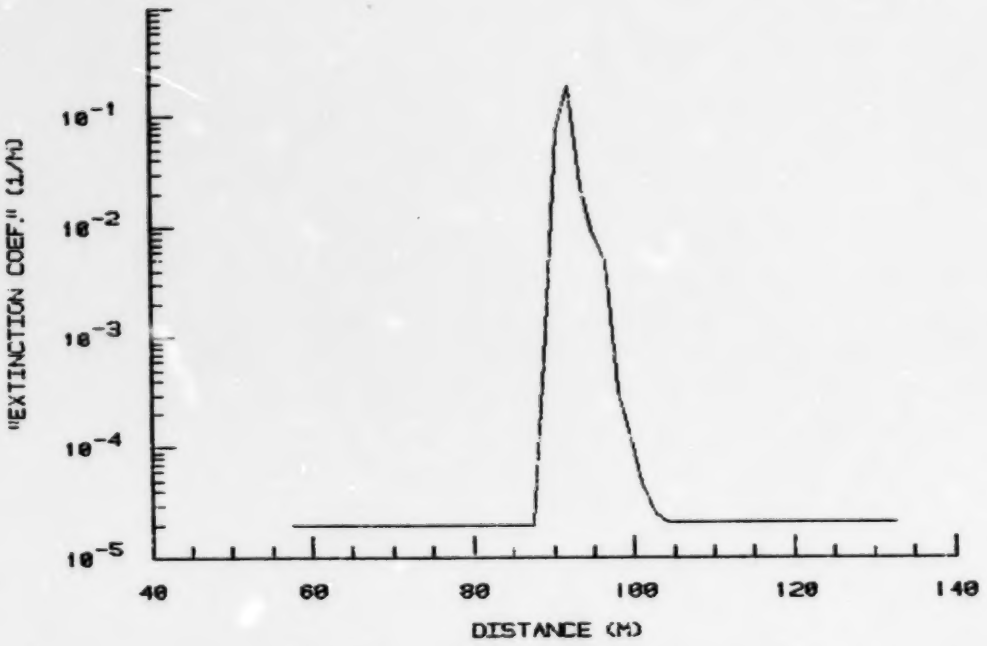

FIGURE 7 - Inversion of a target return

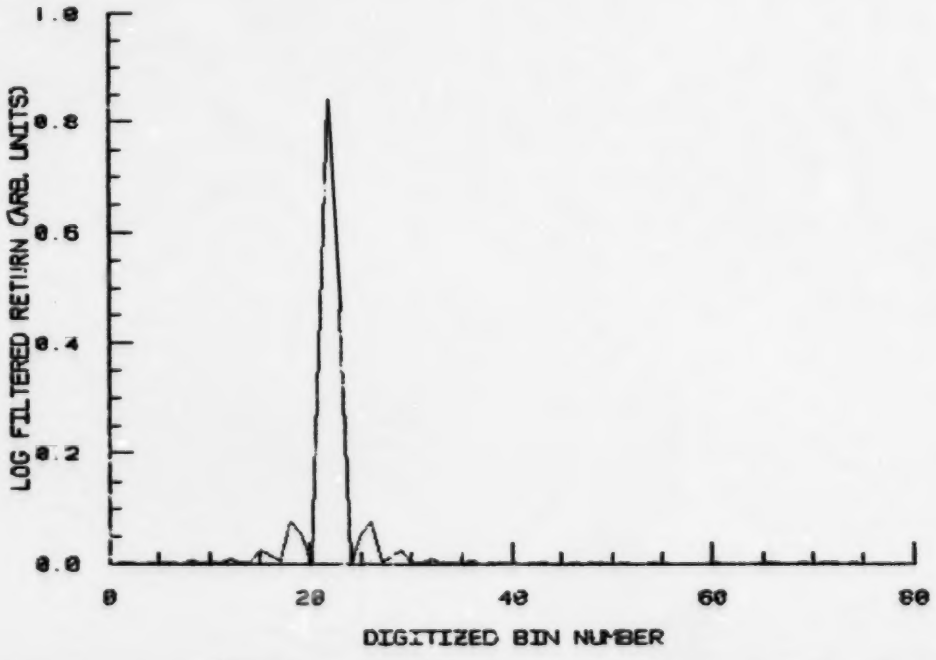

FIGURE 8 - Wiener filter as applied to the target return of Fig. 7

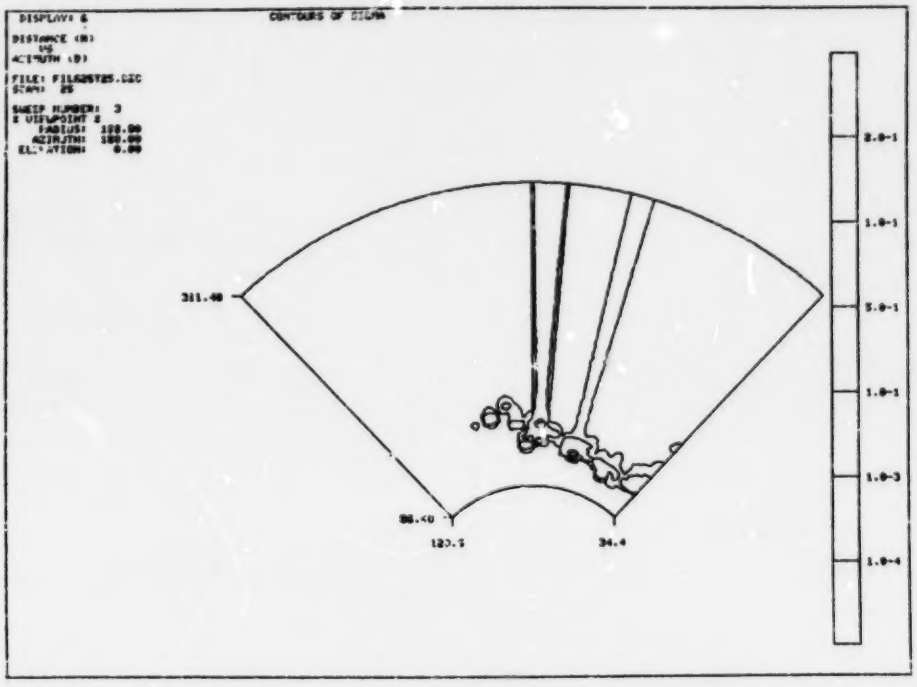

FIGURE 9 - Lidar-produced cloud map without correction of logarithmic amplifier and multi-scattering

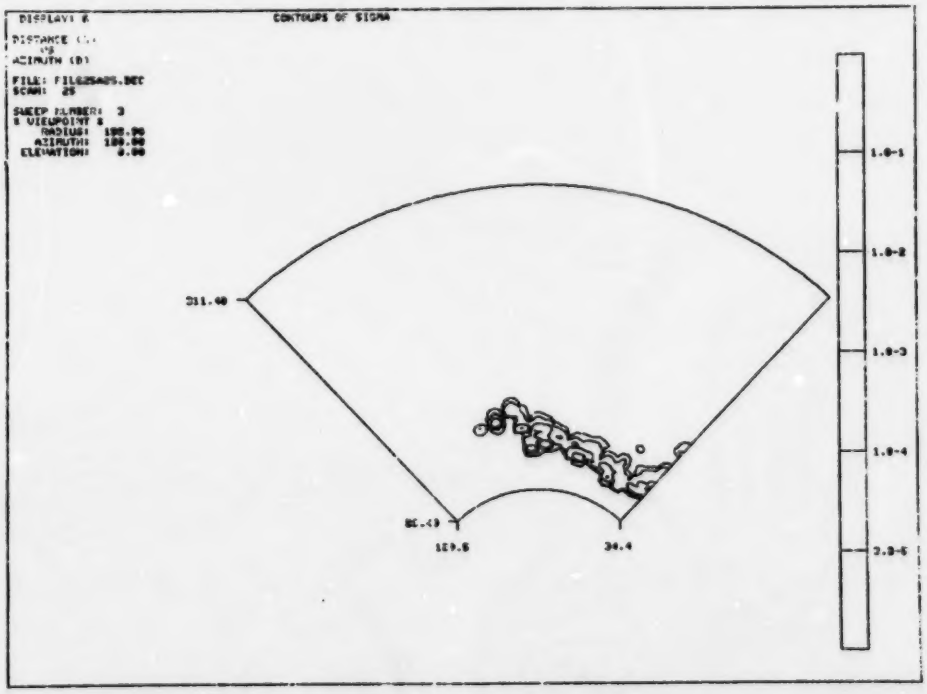

FIGURE 10 - Same cloud map as in Fig. 9, with corrections

The program that produced the examples for this report using the new inversion method guarantees that the integral limit [18] will not be exceeded so that some compensation for multi-scattering will be present. No claim is made here that this compensation is complete or correct.

5.3 Particle Size Distribution

It is difficult to imagine conditions in nonsolid particulate clouds or smokes in which the particle size distribution does not change. Varying humidities will affect the size distribution of hygroscopic particles for example. For burning red phosphorus, the size distribution will become stable only at some distance from the source, even if the humidity is uniform. However, it was shown in Section 4.4 that there is good agreement between the calculation and the photographic evidence. Thus the value of k used cannot vary appreciably from unity since this would change the cloud extent and hence bias Fig. 4, since the inversion would give larger values. This can be clearly seen in Figs. 11a and b, which show a plot of extinction coefficient versus distance for various values of k. Values of k less than unity affect the cloud extent to a greater degree than $k > 1$. Notice that the extinction values are also changed, which would affect the relationships already shown in Fig. 3 and Table I.

A survey of the literature indicates that for most conditions, $k = 1$. Theoretical results (Refs. 7, 29-32) and experimental results (Refs. 8, 17, 33-35) over a variety of materials, particle shapes, and extinction coefficients indicate that this assumption of linearity is excellent. However caution is required since, as indicated by results in Refs. 8, 9, 33, 36-37, effects such as multi-scattering, changes of size distribution (due to humidity or settling, etc.) and index of refraction, and particle shape can cause nonlinearity. Values of $k = 0.66$ have been reported (see Ref. 31 and the references contained therein).

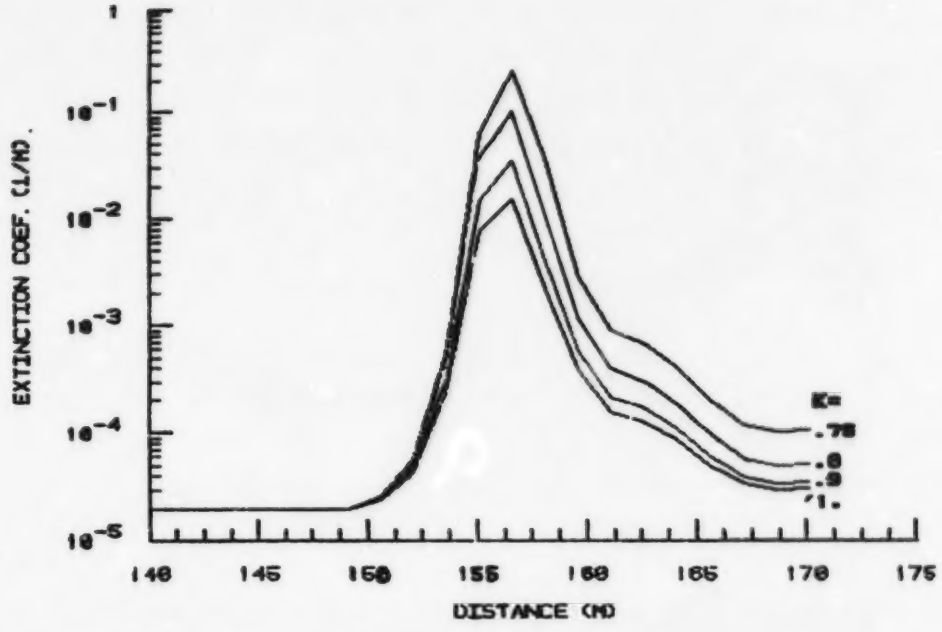

FIGURE 11a - Effect of power law variation in the backscatter-extinction relation on inversion results (k < 1)

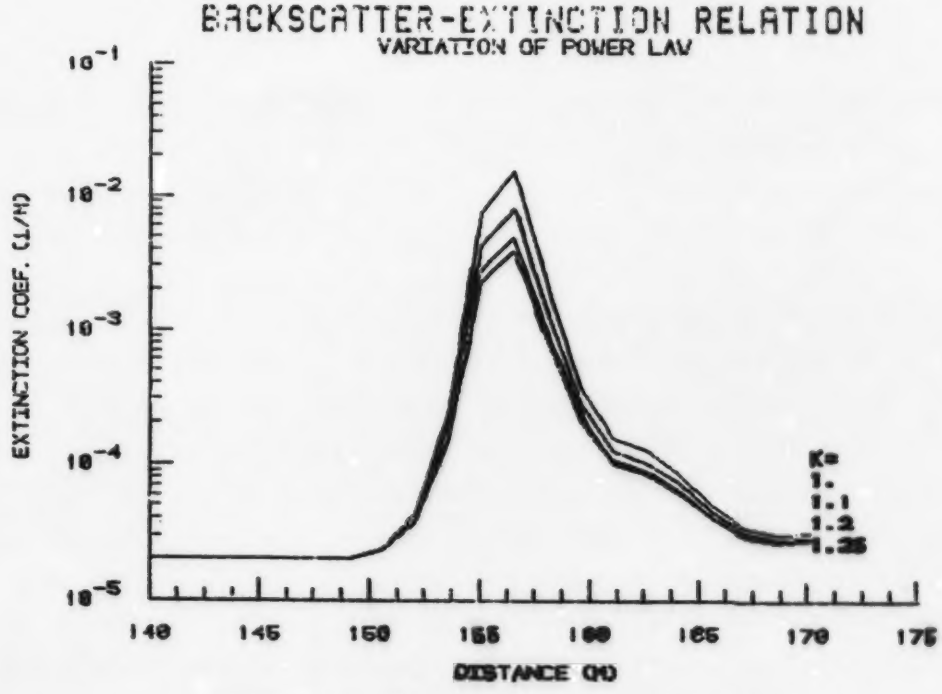

FIGURE 11b - Same as Fig. 11a but k > 1

As mentioned in Section 3.4, the clear air extinction coefficient σ_c can be interpreted as the effective extinction coefficient in order to account for the differences between the proportionality constant d in [6] relating the clear air aerosol to the aerosol under study. The subsequent inversion using the calibration value of σ_c will continue to be valid (under conditions discussed in Section 4.1) unless the constant d in [6] for the material studied changes.

6.0 SUMMARY AND CONCLUSIONS

In this report, a method has been developed that permits the inversion of the lidar equation under a wide variety of conditions. This solution overcomes instability in both the high and low visibility cases, in contrast with the solutions proposed by Klett and Lentz (Refs. 1, 2), by normalizing the signal by a clear air return and considering multi-scattering. This solution is designed to invert the lidar equation more accurately and with less computation.

It is demonstrated that there is a theoretical limit to the total power received (normalized integrated backscatter) in a return signal which provides:

1. a check on the validity of the lidar equation;

2. a check on the system itself;

3. transmission at any point, independent of the inversion;

4. that the transmission is obtained after only one numerical integration instead of two and is therefore more accurate, as a consequence of #3; and

5. a new inversion method without the need for a guess or a need for iteration to yield convergence to some constraint.

The solution is validated in a number of ways, including:

1. comparison with Klett's method (Refs. 1 and 2);

2. comparison of predicted and measured transmissions;

3. comparison of calculated concentrations with measured concentration values from the literature; and

4. cloud extent.

It is also shown that calibrating the lidar signal with a reference signal (in this report, a clear air signal) makes the r^2 correction unnecessary and considerably improves the ability to detect a weak signal amongst significant system noise. As a result, the values of extinction produced by the inversion are independent of the starting point of the inversion.

7.0 ACKNOWLEDGEMENTS

The author wishes to thank Mr. R.E. Kluchert for encouragement and many helpful discussions, as well as Dr. W.G. Tam for help concerning the theory of multi-scattering.

8.0 REFERENCES

1. Klett, J.D., "Stable Analytical Inversion Solution for Processing Lidar Returns", Applied Optics, Vol. 20, No. 2, pp. 211-220, 1981.

2. Lentz, W.J., "The Visioceilometer: A Portable Visibility and Cloud Ceiling Height Lidar", Atmospheric Sciences Lab., TR-0105, January 1982.

3. Hitschfeld, W. and Bordan, J., "Errors Inherent in the Radar Measurement of Rainfall at Attenuating Wavelengths", J. of Meteorology, Vol. 11, pp. 58-67, 1954.

4. Evans, B.T.N., "Field Evaluation of a Canadian Laser Cloud Mapper and Candidate IR Screening Aerosols", Smoke/Obscurants Symposium VI, Unclassified Section, Harry Diamond Labs., Adelphi, Md., April 1982.

5. Chandrasekhar, S., "Radiative Transfer", Dover Pub. Inc., New York, 1960.

6. Uthe, E.E., "Evaluation of the Propagation Environments using Laser Radar Techniques", Office of the Director of Defense Research and Engineering Propagation Workshop, USAF Academy, Colorado, 5-9 December 1976.

7. Carrier, L.W., Cato, A. and Von Essen, K.J., "The Backscattering and Extinction of Visible and Infrared Radiation by Selected Major Cloud Models", J. of Applied Optics, Vol. 6, No. 7, pp. 1209-1216, 1967.

8. Sztankay, Z.G., McGuire, D., Griffin, J., Hattery, W., Martin, G. and Wetzel, G., "Near-IR Extinction, Backscatter, and Depolarization of Smoke Week III Aerosols", Proceedings of the Smoke/Obscurants Symposium V, Harry Diamond Labs., Adelphi, Md., April 1981.

9. De Leeuw, G., "Mie Scattering on Particle Size Distributions. Influence of Size Limits and Complex Refractive Index on the Calculated Extinction and Backscatter Coefficients", Physics Laboratory TNO, PHL 1982-50, The Netherlands, 1982.

10. Kohl, R.H., "Discussion of the Interpretation Problem Encountered in Single-Wavelength Lidar Transmissometers", J. of Applied Meteorology, Vol. 17, pp. 1034-1038, July 1978.

11. Fernald, F.G., Herman, B.M. and Reagan, J.A., "Determination of Aerosol Height Distributions by Lidar", J. of Applied Meteorology, Vol. 11, pp. 482-489, 1972.

12. Uthe, E., Private Communication.

13. Carswell, A., Private Communication.

14. Fujimura, S.F., Warren, R.E. and Lutomirski, R.F., "Lidars for Smoke and Dust Cloud Diagnostics", Pacific-Sierra Research Corp., Contract DAAK20-70-C-0040, May 1980.

15. Kunkel, K.E. and Weinman, J.A., "Monte Carlo Analysis of Multiple Scattered Lidar Returns", Journal of the Atmospheric Sciences, Vol. 33, pp. 1772-1781, 1976.

16. Smith, R.B., Carswell, A.I., Houston, J.D., Pal, S.R. and Greiner, B.C., "Multiple Scattering Effects on Backscattering and Propagation of Infrared Laser Beams in Dense Military Screening Clouds", Optech Inc. Final Report, Contract No. 8SD81-00084, February 1983.

17. Lamberts, C.W., "LIDAR. A Statistical Approach", Physics Laboratory, The Hague, Netherlands, PHL 1978-31, 1978.

18. Bruce, D., Bruce, C.W., Yee, Y.P., Chenzl, L. and Burket, H., "Experimentally Determined Relationship between Extinction Coefficients and Liquid Water Content", Applied Optics, Vol. 19, No. 19, pp. 3355-3360, 1980.

19. Pinnick, R.G., Jennings, S.G., Chylek, P. and Auvermann, H.J., "Verification of a Linear Relation between IR Extinction, Absorption and Liquid Water Content of Fogs", Journal of the Atmospheric Sciences, Vol. 36, pp. 1577-1586, 1979.

20. Stuebing, E.W., "Relative Humidity Dependence of the Infrared Extinction by Aerosol Clouds of Phosphoric Acid", Proc. of the Smoke/Obscurants Symposium III, Harry Diamond Labs., Adelphi, Md., April 1979.

21. Allen, G., "Attenuation of Infrared Laser Radiation by HC, FS, WP, and Fog-Oil Smokes", Edgewood Arsenal, Md., EATR 4405, 1970.

22. Smith, M.D., Jones K. and Kittikul, P., "A Data Reduction Technique for Field Data", Proc. of the Smoke/Obscurants Symposium V, Harry Diamond Labs., Adelphi, Md., pp. 97-125, 1981.

23. Farmer, W.M., Schwartz, F.A., Morris, R.D., Hornkohl, J.O. and Binkley, M.A., "Field Characterization of Phosphorus Smokes using Spectral Transmittance and Real-Time Concentration Measurements", Proc. SPIE-Int. Soc., Optical Engineering, Vol. 277, pp. 48-57, 1981.

24. Boulter, J.F., "Application of Deconvolution Filtering to Improve the Range Resolution of a Ladar Target Imaging System", DREV TN-2120/74, March 1974, UNCLASSIFIED

25. Evans, B.T.N., Cerny, E. and Gagné, R., "Computerized Lidar Displays of IR Obscuring Aerosols", Proc. Smoke/Obscurants Symposium VII, Harry Diamond Labs., Adelphi, Md., April 1983.

26. Tam, W.G., "Multiple Scattering Corrections for Atmospheric Aerosol Extinction Measurements", Applied Optics, Vol. 19, No. 13, pp. 2090-2092, 1980.

27. Pal, S.R. and Carswell, A.I., "Multiple Scattering in Atmospheric Cloud: Lidar Observations", Applied Optics, Vol. 15, No. 8, pp. 1990-1995, 1976.

28. Samokhvalov, I.V., "Double-Scattering Approximation of Lidar Equation for Inhomogeneous Atmosphere", Optics Letters, Vol. 4, No. 1, pp. 12-14, 1979.

29. Ross, D.A. and Kuriger, N.L., "Expected Lidar Return from Tornado Clouds", Applied Optics, Vol. 15, No. 12, pp. 2958-2959, 1976.

30. Herrman, H., Kopp, F. and Werner, C., "Remote Measurements of Plume Dispersion over Sea Surface using the DFVLR Minilidar", Optical Engineering, Vol. 20, No. 5, pp. 759-764, 1981.

31. Twomey, S. and Howell, H.B., "The Relative Merit of White and Monochromatic Light for the Determination of Visibility by Back-Scattering Measurements", Applied Optics, Vol. 4, No. 4, pp. 501-506, 1965.

32. Bird, R.E., "Extinction and Backscattering by Fog and Smoke in the 0.33 to 12.0 Micrometer Wavelength Region", NWC TR-5850, Naval Weapons Center, China Lake, Cal., 1976.

33. Waggoner, A.P., Ahlguist, N.C. and Charlson, R.J., "Measurement of the Aerosol Total Scatter-Backscatter Ratio", Applied Optics, Vol. 11, No. 12, pp. 2886-2889, 1972.

34. Kohl, R., Course on Atmospheric Optics Notes, University of Tennessee, Tullahoma, Tennessee, March 1982.

35. Pinnick, R.G., Jennings, S.G., Chylek, P. and Ham, C., "Backscatter and Extinction in Water Clouds", Tenth International Laser Radar Conference, Silver Spring, MD, 1980.

36. Sztankay, Z.G., "Measurement of the Localized Optical Characteristics of Natural Aerosols, Smoke, and Dust", Proc. of the Smoke/Obscurants Symposium II, Harry Diamond Labs., Adelphi, Md., April 1978.

37. Fenn, R.W., "Correlation between Atmospheric Backscattering and Meteorological Visual Range", Applied Optics, Vol. 5, No. 2, pp. 293-295, 1966.

APPENDIX A

The Effects of Clear Air Calibration

In Section 3.4, where the new inversion method is developed, the lidar return signal is divided by a clear air return (or by any other reference signal). In so doing, the data are immediately corrected for $1/r^2$ attenuation, the system constant F(r), and most system noise. In this appendix, the sensitivity gained due to the latter effect will be discussed.

Two histograms are given in Figs. A1 and A2 of the same lidar return showing the distribution, after inversion, of extinction coefficients. Here Fig. A1 is the inversion with just the $1/r^2$ correction, while Fig. A2 is the same inversion but using the clear air return for calibration. In both cases, the shot has been corrected for laser power signal with respect to the calibrating shot. Also, the clear air extinction coefficient was taken to be 2.0×10^{-5} m^{-1}. For this case, the standard deviation is essentially halved by using the calibrating shot. And, significantly, Fig. A2 allows for the detection of a very weak return of the cloud while, from the statistics of the noise, Fig. A1 does not. Indeed, the one point in Fig. A2 (at 2.6×10^{-5} m^{-1}) shows that the cloud is more than eight standard deviations from the mean whereas it is only three standard deviations from the mean in Fig. A1 (at 2.3×10^{-5} m^{-1}).

Figure A3 is the distribution for the extinction values of over 1200 clear air extinction coefficients. In this way, an excellent value of the standard deviation of the clear air extinction in the data can be derived, enabling the detection of very weak returns. For example, if an extinction value is over three standard deviations

higher than the clear air median, the probability that the discrepancy is due to noise, with the present data, is less than 0.27%. In this way it is possible to distinguish between what is signal and what is noise.

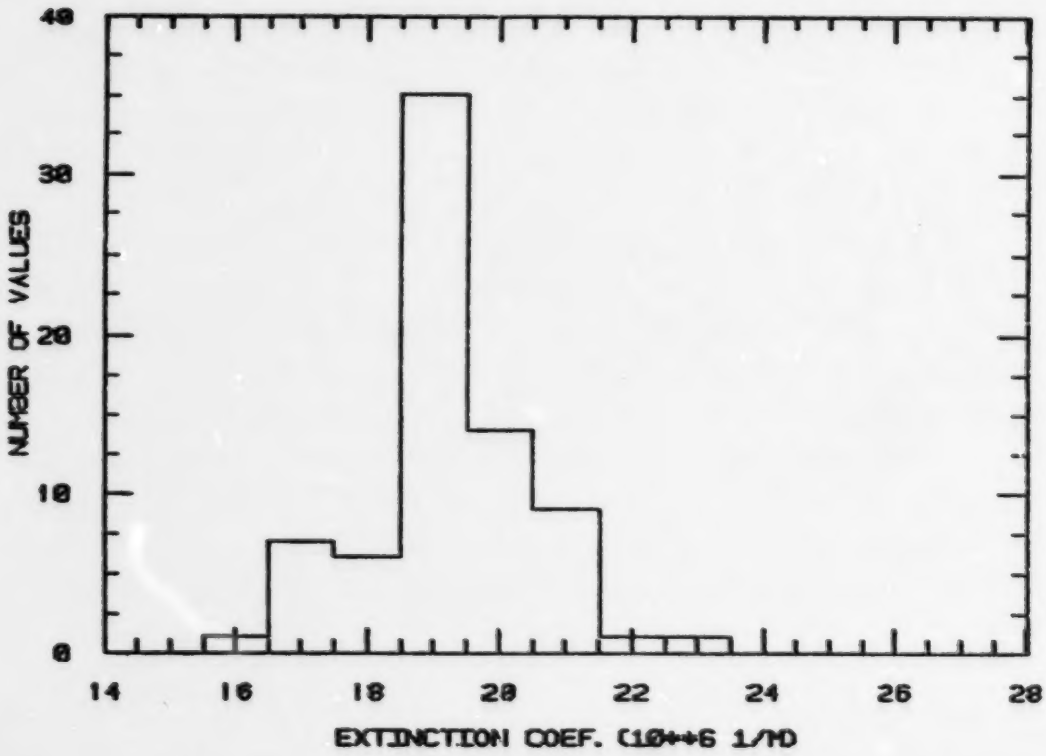

FIGURE A1 - Distribution of extinction coefficients without clear air normalization

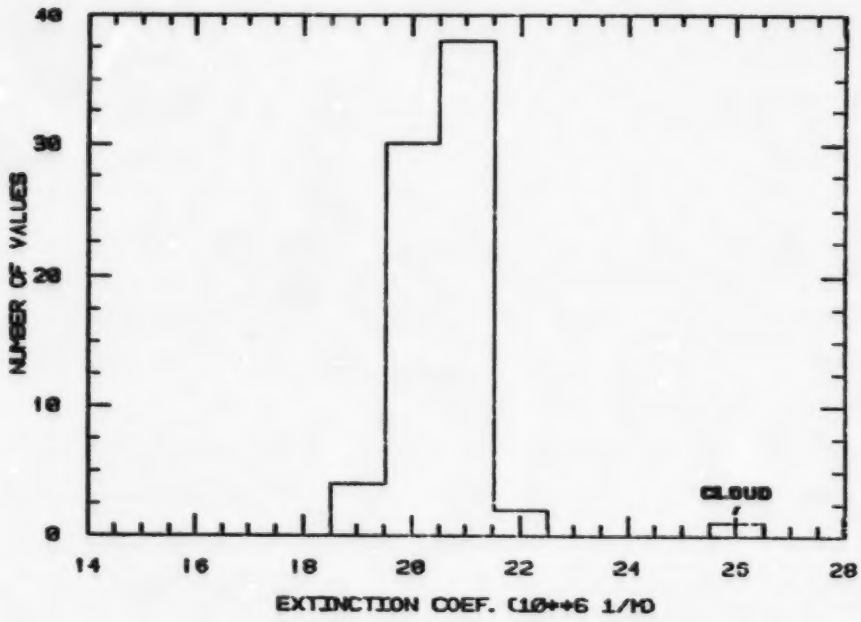

FIGURE A2 - Distribution of extinction coefficients with clear air normalization

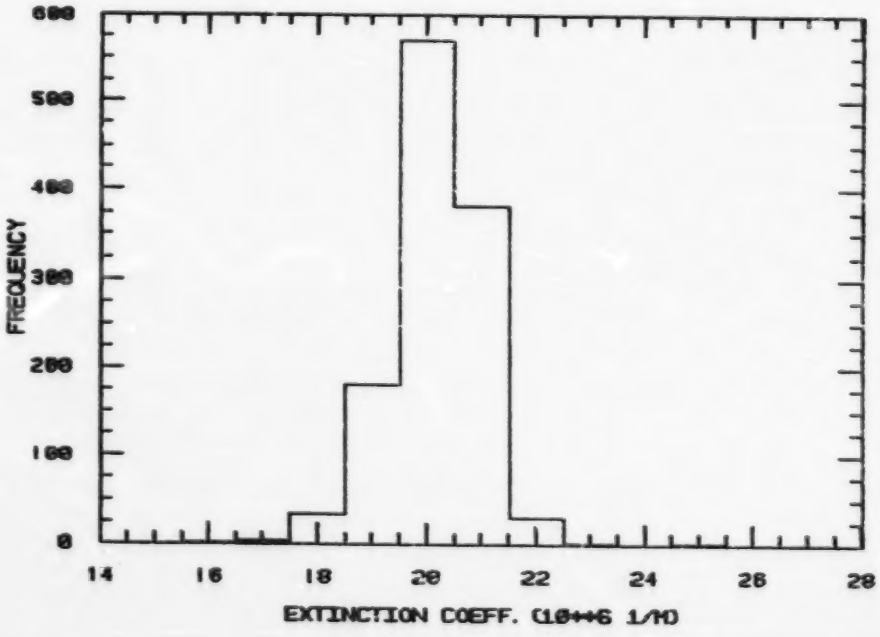

FIGURE A3 - Distribution of over 1200 extinction coefficients with clear air normalization

APPENDIX B

Correction for the Logarithmic Amplifier Response

As shown in Fig. 2, the logarithmic amplifier response is far from ideal, and the use of digital filters can be difficult (as in the one attempt discussed in Section 5.1). The method used in the current inversion program to correct for this response is to multiply the return signal by a factor less than unity if the cloud is sufficiently dense. This factor decreases continuously as the integrated backscatter gets larger. The actual factor used is T^{-z} where T is the optical depth and z is the adjustable parameter.

The program halts if too much correction is required, assuming that calculation beyond this point produces meaningless information. The amount of correction needed and when to halt the program must be empirically decided. This is done by comparison with transmission values and cloud extent. Note that the amount adjusted for is controlled by a single parameter z and that this is made a constant. A multi-parameter model was felt to be too flexible, i.e. it could be made to fit almost any condition. For the program used here, a value of $z = 0.8$ was found to be reasonable; that is, it was a good fit with the observed transmissions.

APPENDIX C

Numerical and Digitization Errors

In calculating the inversion, a numerical integration must be performed, with its inherent errors. Furthermore, the digitization of the analog signal obtained by the LCM also places an unavoidable error in the data, which is due to the finite word size of the digitizer. The purpose of this appendix is to estimate the importance of these two errors. The errors produced in the integration and digitization of the artificial signal shown in Fig. C1 will be discussed. This is mathematically a simple representation of a range-corrected lidar return signal, with the height H and an offset D being adjustable. The parameter H is taken as a relative change between the clear air signal and the plateau height and D is in units of the digitization rate.

The error will be taken here as the difference between the theoretical area under the curve (to the first data bin after the signal height H) and the numerically derived area.

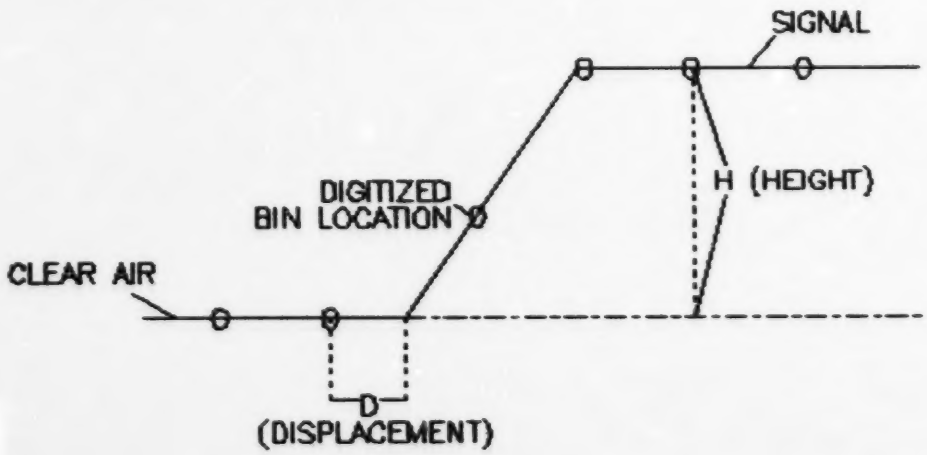

FIGURE C1 - Artificial lidar return used for estimating numerical and digitization errors

TABLE CI

Variation of Integration Error with Offset and Signal Height (Infinite Word Size)

	Signal Height (H)			
	1	10	100	1000
OFFSET (D) 0	0	<0.5	<0.5	<0.5
0.1	0	3	8	10
0.5	0	13	55	90
0.9	0	30	150	470

TABLE CII

Variation of Digitization Error with Offset and Signal Height (8-Bit Word Size)

	Signal Height (H)			
	1	10	100	1000
OFFSET (D) 0	0	1	50	90
0.1	0	20	80	110
0.5	0	30	120	300
0.9	0	40	170	800

TABLE CIII

Variation of Digitization Error with Offset and Signal Height (16-Bit Word Size)

	Signal Height (H)			
	1	10	100	1000
OFFSET (D) 0	0	0.8	8	10
0.1	0	13	40	70
0.5	0	20	90	200
0.9	0	30	150	600

C1.1 Integration Errors

Both the offset D and height H of a lidar return can vary and, in the case of a dense smoke, H can vary considerably even within the best spatial resolution available to the LCM (1.5 m). For the program of this report, Simpson's Rule was used since it is simple to apply and the theoretical error term is of the fourth order in the digitization rate. This is the most accurate method for numerical integration under conditions of a uniform digitization rate and at the same time gives an integrated value (in combination with the trapezoidal rule) at every digitized point. Table CI lists the errors associated with the numerical integration of Fig. C1 for ranges of offset from 0-0.9, signal heights of 1 to 1000 and an infinite digitization word size. It is evident that large offsets can be tolerated only if the signal remains relatively small.

C1.2 Digitization Errors

The digitization errors have two sources other than that which is included in the numerical integration error. These are the finite word length and round-off error. In the calculation done here, the two are treated together. Tables CII and CIII are the errors obtained by varying the word size, signal height H, and the offset D. It can be seen that for a certain combination of H and D, there is a small range of word sizes in which the error increases rapidly.

C2.0 DISCUSSION OF ERRORS

The LCM digitizes lidar data with an 8-bit word size. In addition, the maximum observed relative change in signal strength due to red phosphorus or HC smokes is 20 times over 1.5 m. Assuming, as a rough approximation, that the signal increases linearly in the interval, the maximum error due to numerical integration occurs for an offset of 0.5 when the signal has increased 10 times. Table CI then gives a value of 13% for the error due to numerical integration. For the same case, the digitization error becomes 15%. In general, the relative change in the signal is considerably less than 20 times and errors less than 5-10% seem to be more likely. The integration over the total signal will have less error due to less signal variation and some error cancellation.

It is clear from the above-mentioned information that computational errors depend strongly on the signal variation. Therefore the inversion method presented in this report incurs less error than the other methods since transmission can be derived from one integral (the normalized integrated backscatter) instead of two (i.e. the normalized integrated backscatter and the integral of extinction values).

APPENDIX D

FORTRAN Program Listing of AGILE

```
C                              AGILE
C    (AUTOMATICALLY GENERATED INVERSION OF THE LIDAR EQUATION)
C
C    INITIALIZATION
C
C    C(I)---CLEAR AIR RAW DATA ARRAY (BECOMES NORMALIZED LIDAR
C           RETURN)
C    CA-----CLEAR AIR EXTINCTION VALUE
C    CA1----CA1=1/CA
C    C1(I)--CLEAR AIR ARRAY
C    K------LAST BIN OF RETURN CONSIDERED
C    N------NUMBER OF BINS CONSIDERED PER LIDAR RETURN
C    P(I)---LINEARIZED RAW RETURN DATA ARRAY
C    P1(I)--RAW LIDAR RETURN DATA ARRAY
C    R------DIGITIZED BIN TO BIN DISTANCE
C    R1-----CONSTANT USED IN NUMERICAL INTEGRATION
C    SIG(I)-CALCULATED  EXTINCTION COEFFICIENT
C    SUM(I)-NORMALIZED INTEGRATED BACKSCATTER ARRAY
C    T(I)---TRANSMISSION AT THE ITH BIN
C    ZN-----LOG-AMP CORRECTION PARAMETER
C    ZZ-----NOISE LEVEL THRESHOLD
C
      REAL*4 SIG(150),SUM(150),T(150),P(150),C(150),P1(150),C1(150)
      DATA SIG,T/300*0./
      R=3.0
      R1=R*2./3.
      N=76
      CA=.00002
      CA1=1./CA
      ZN=.8
      ZZ=0.
C
C    READ  IN DIGITIZED LIDAR RETURN DATA
C
```

```
C
C    READ  IN DIGITIZED LIDAR RETURN DATA
C
       DO 1 I=1,N
       READ(5,1000) P1(I)
     1 READ(8,1000) C(I)
C
C    LINEARIZE RAW DATA
C
     4 DO 5 I=1,N
       C(I)=10**(.026*C(I)-6.6)
     5 P(I)=10**(.026*P1(I)-6.6)
C
C    FIND BIN WHICH IS BELOW NOISE THRESHOLD  IF THERE IS ONE
C
     6 K=0
       DO 15 I=1,N
       IF(K) 15,16,15
    16 IF(P(I).LT.ZZ) K=I-1
    15 CONTINUE
       IF(K.EQ.0) K=N
C
C    CORRECTION FOR LOW RETURN SIGNAL
C
       CC=P(1)/C(1)
       IF(CC.GT.1.) CC=1.
C
C    CLEAR AIR CORRECTION
C
       DO 8 I=1,K
       C(I)=(P(I)/(C(I)*CC))
     8 C1(I)=C(I)
C
C    SIMPSON'S/TRAPEZIOD INTEGRATION UNTIL ONE OPTICAL DEPTH
```

```
C
C   SIMPSON'S/TRAPEZIOD INTEGRATION UNTIL ONE OPTICAL DEPTH
C
      SUM(1)=0.
      SUM(2)=R*(C(1)+C(2))
      DO 111 I=3,K-1,2
      SUM(I)=SUM(I-2)+(C(I-2)+4.*C(I-1)+C(I))*R1
      IF(SUM(I).GT.CA1*.6) GOTO112
      SUM(I+1)=SUM(I)+(C(I)+C(I+1))*R
  111 IF(SUM(I+1).GT.CA1*.6) GOTO114
      K2=K-2*(K/2)
      IF(K2.EQ.0) GOTO105
      SUM(K)=SUM(K-2)+(C(K-2)+4.*C(K-1)+C(K))*R1
      GOTO105
  114 I=I+1
  112 K1=I-1
C
C   SIMPSON'S/TRAPEZIOD INTEGRATION WITH LOG-AMP AND
C   MULTI-SCATTER CORRECTION
C
      DO 102 I=K1,K-1,2
      C(I)=C(I)*(1.-(SUM(I-1)*CA)**ZN)
      IF(C(I).GE.0.005) GOTO101
  104 K=I-1
      GOTO115
  103 K=I
      GOTO115
  101 SUM(I)=SUM(I-2)+(C(I-2)+4.*C(I-1)+C(I))*R1
      IF(SUM(I).GT.SUM(I-1)) GOTO108
      SUM(I-1)=SUM(I-1)-C(I-2)*R1/2.
  108 IF(SUM(I).GE.CA1) GOTO104
      C(I+1)=C(I+1)*(1.-(SUM(I)*CA)**ZN)
      IF(C(I+1).LT.0.005) GOTO104
      SUM(I+1)=SUM(I)+(C(I)+C(I+1))*R
```

```
  102 IF(SUM(I+1).GE.CA1) GOTO103
      K2=(K-K1)-2*((K-K1)/2)
      IF(K2.EQ.1) GOTO115
      C(K)=C(K)*(1.-(SUM(K-1)*CA)**ZN)
      IF(C(K).LT.0.005) GOTO106
      SUM(K)=SUM(K-2)+(C(K-2)+4.*C(K-1)+C(K))*R1
      IF(SUM(K).LE.CA1) GOTO109
  106 K=K-1
  109 IF(SUM(K).GT.SUM(K-1)) GOTO115
      SUM(K-1)=SUM(K-1)-C(I-2)*R1/2.
  115 CONTINUE
C
C   LIDAR EQUATION INVERSION
C
  105 DO 110 I=1,K
      T(I)=(1-SUM(I)*CA)**(.5)
  110 SIG(I)=C(I)/(CA1-SUM(I))
C
C   WRITE RESULTS
C
      WRITE(6,1004)
      DO 301 I=1,K
  301 WRITE(7,1007) R*I-36.0,SIG(I),100.*T(I),SUM(I),C(I),C(I)/C1(I),
     1P(I),P1(I)
 1000 FORMAT(1X,F6.3)
 1004 FORMAT(2X,'R(M)',3X,'COEF.',3X,'TRANS.',4X,'INTEGRAL',
     16X,'NSIG',2X,'MS CORR.',2X,'LIN P',2X,'LOG P'/)
 1007 FORMAT(1X,F5.1,F9.7,F8.3,F12.2,F10.3,F9.3,F9.6,F6.1)
      STOP
      END
```

R(M)	COEF.	TRANS.	INTEGRAL	NSIG	MS CORR.	LIN P	LOG P
57.6	.0000286	100.000	.00	1.432	1.000	.001570	146.0
59.1	.0000254	99.996	4.05	1.271	1.000	.001164	141.0
60.6	.0000225	99.992	7.64	1.127	1.000	.000721	133.0
62.1	.0000254	99.989	11.24	1.271	1.000	.000721	133.0
63.6	.0000254	99.985	15.12	1.271	1.000	.000916	137.0
65.1	.0000270	99.981	19.65	1.349	1.000	.001164	141.0
66.6	.0000287	99.977	23.22	1.432	1.000	.000813	135.0
68.1	.0000287	99.972	27.52	1.432	1.000	.000568	129.0
69.6	.0000254	99.968	31.65	1.271	1.000	.000640	131.0
71.1	.0000270	99.964	35.68	1.349	1.000	.000363	136.0
72.6	.0000287	99.960	39.75	1.432	1.000	.000813	135.0
74.1	.0000304	99.956	44.18	1.521	1.000	.000640	131.0
75.6	.0000140	99.952	47.96	.698	1.000	.000535	128.0
77.1	.0000240	99.949	50.81	1.197	1.000	.000535	128.0
78.6	.0000240	99.945	54.64	1.197	1.000	.000535	128.0
80.1	.0000240	99.942	58.24	1.197	1.000	.000504	127.0
81.6	.0000240	99.938	61.83	1.197	1.000	.000504	127.0
83.1	.0000254	99.934	65.53	1.271	1.000	.000447	125.0
84.6	.0000240	99.931	69.30	1.197	1.000	.000396	123.0
86.1	.0000240	99.927	72.89	1.197	1.000	.000447	125.0
87.6	.0000240	99.923	76.48	1.197	1.000	.000504	127.0
89.1	.0000255	99.920	80.18	1.271	1.000	.000352	121.0
90.6	.0000255	99.916	84.03	1.271	1.000	.000331	120.0
92.1	.0000240	99.912	87.73	1.197	1.000	.000373	122.0
93.6	.0000270	99.909	91.44	1.349	1.000	.000474	126.0
95.1	.0000270	99.904	95.48	1.349	1.000	.000396	123.0
96.6	.0000270	99.900	99.53	1.349	1.000	.000331	120.0
98.1	.0000255	99.896	103.46	1.271	1.000	.000331	120.0
99.6	.0000270	99.893	107.31	1.349	1.000	.000373	122.0
101.1	.0000270	99.889	111.36	1.349	1.000	.000373	122.0
102.6	.0000255	99.885	115.33	1.271	1.000	.000331	120.0
104.1	.0000226	99.881	118.92	1.127	1.000	.000277	117.0

105.6	.0000226	99.878	122.23	1.127	1.000	.000277	117.0
107.1	.0000240	99.874	125.72	1.197	1.000	.000312	119.0
108.6	.0000240	99.871	129.34	1.197	1.000	.000312	119.0
110.1	.0000271	99.867	133.16	1.349	1.000	.000312	119.0
111.6	.0000271	99.863	137.29	1.349	1.000	.000294	118.0
113.1	.0000255	99.859	141.22	1.271	1.000	.000294	118.0
114.6	.0000240	99.855	144.91	1.197	1.000	.000294	118.0
116.1	.0000271	99.851	148.73	1.349	1.000	.000294	118.0
117.6	.0000305	99.847	153.03	1.521	1.000	.000312	119.0
119.1	.0000344	99.842	157.88	1.714	1.000	.000352	121.0
120.6	.0000437	99.836	163.58	2.178	1.000	.000447	125.0
122.1	.0000844	99.827	173.16	4.207	1.000	.000863	136.0
123.6	.0002074	99.807	192.92	10.328	1.000	.002118	151.0
125.1	.0005410	99.751	248.78	26.915	1.000	.004898	165.0
126.6	.0016923	99.604	394.85	83.946	1.000	.013552	182.0
128.1	.0086532	98.838	1154.77	422.668	1.000	.072443	210.0
129.6	.0410946	95.857	4057.46	1887.990	1.000	.387257	238.0
131.1	.1425368	84.593	14228.19	5098.797	.866	1.009252	254.0
132.6	.1657863	67.116	27477.31	3733.950	.634	.704692	248.0
134.1	.0577949	54.548	35122.62	859.836	.381	.364753	237.0
135.6	.0642689	49.785	37607.09	796.478	.246	.625172	246.0
137.1	.0838307	44.708	40006.16	837.790	.204	.794327	250.0
138.6	.1417682	37.960	42795.00	1021.438	.163	1.009252	254.0
140.1	.1468316	29.736	45578.86	649.161	.117	.843334	251.0
141.6	.0536728	25.261	46809.46	171.244	.071	.387257	238.0
143.1	.0193526	24.604	46973.08	60.092	.051	.188799	226.0
144.6	.0187935	23.981	47143.73	53.679	.049	.157761	223.0
146.1	.0138276	23.388	47285.42	37.536	.046	.116950	218.0
147.6	.0079205	22.922	47372.93	20.808	.044	.064269	208.0
149.1	.0035771	22.736	47415.43	9.245	.042	.029512	195.0
150.6	.0017293	22.645	47435.95	4.434	.042	.015276	184.0
152.1	.0006219	22.610	47444.08	1.590	.041	.005861	168.0
153.6	.0003027	22.594	47447.54	.773	.041	.002692	155.0
155.1	.0001873	22.587	47449.16	.478	.041	.001479	145.0

156.6	.0001232	22.582	47450.34	.314	.041	.000973	138.0
158.1	.0000810	22.578	47451.89	.206	.041	.000679	132.0
159.6	.0000637	22.576	47451.64	.162	.041	.000535	128.0
161.1	.0000445	22.574	47452.06	.113	.041	.000373	122.0
162.6	.0000419	22.573	47452.39	.107	.041	.000331	120.0
164.1	.0000395	22.571	47452.70	.101	.041	.000312	119.0
165.6	.0000311	22.570	47452.97	.079	.041	.000261	116.0
167.1	.0000230	22.569	47453.18	.059	.041	.000193	111.0
168.6	.0000192	22.568	47453.34	.049	.041	.000152	107.0
170.1	.0000245	22.568	47453.49	.062	.041	.000171	109.0

STOP 0

DREV R-4343/84 (UNCLASSIFIED)

Research and Development Branch, DND, Canada.
DREV, P.O. Box 8800, Courcelette, Que. G0A 1R0

"On the Inversion of the Lidar Equation" by B.T.N. Evans

A modified form of the Klett inversion method of the lidar equation is developed. The accuracy of this inversion method is explored and validated. Unlike previous inversions, this one does not require making a guess for each lidar return to initiate the calculation.

Included are discussions of the other inversion methods. The assumptions contained in the single-scatter lidar equation and in the inversion method are outlined as is their relative importance. Special attention is given to the backscatter versus total extinction relation, multi-scattering and non-ideal detector response.

DREV R-4343/84 (UNCLASSIFIED)

Research and Development Branch, DND, Canada.
DREV, P.O. Box 8800, Courcelette, Que. G0A 1R0

"On the Inversion of the Lidar Equation" by B.T.N. Evans

A modified form of the Klett inversion method of the lidar equation is developed. The accuracy of this inversion method is explored and validated. Unlike previous inversions, this one does not require making a guess for each lidar return to initiate the calculation.

Included are discussions of the other inversion methods. The assumptions contained in the single-scatter lidar equation and in the inversion method are outlined as is their relative importance. Special attention is given to the backscatter versus total extinction relation, multi-scattering and non-ideal detector response.

DREV R-4343/84 (UNCLASSIFIED)

Research and Development Branch, DND, Canada.
DREV, P.O. Box 8800, Courcelette, Que. G0A 1R0

"On the Inversion of the Lidar Equation" by B.T.N. Evans

A modified form of the Klett inversion method of the lidar equation is developed. The accuracy of this inversion method is explored and validated. Unlike previous inversions, this one does not require making a guess for each lidar return to initiate the calculation.

Included are discussions of the other inversion methods. The assumptions contained in the single-scatter lidar equation and in the inversion method are outlined as is their relative importance. Special attention is given to the backscatter versus total extinction relation, multi-scattering and non-ideal detector response.

DREV R-4343/84 (UNCLASSIFIED)

Research and Development Branch, DND, Canada.
DREV, P.O. Box 8800, Courcelette, Que. G0A 1R0

"On the Inversion of the Lidar Equation" by B.T.N. Evans

A modified form of the Klett inversion method of the lidar equation is developed. The accuracy of this inversion method is explored and validated. Unlike previous inversions, this one does not require making a guess for each lidar return to initiate the calculation.

Included are discussions of the other inversion methods. The assumptions contained in the single-scatter lidar equation and in the inversion method are outlined as is their relative importance. Special attention is given to the backscatter versus total extinction relation, multi-scattering and non-ideal detector response.

CRDV R-4343/84 (NON CLASSIFIE)

Bureau - Recherche et Développement, MDN, Canada.
CRDV, C.P. 8800, Courcelette, Qué. G0A 1R0

"Méthode d'inversion de l'équation lidar" par B.T.N. Evans

On a modifié la méthode d'inversion développée par Klett pour l'équation lidar. La validité et l'exactitude de cette nouvelle méthode sont démontrées. Contrairement aux méthodes déjà connues, la modification permet d'éviter l'emploi d'une estimation pour déterminer l'extinction à chaque retour du rayonnement lidar.

On discute aussi des autres méthodes d'inversion. On souligne l'importance des hypothèses dans le développement de l'équation lidar pour la diffusion unique et la méthode d'inversion. On accorde une attention spéciale à la relation entre la rétrodiffusion et l'extinction totale, à la diffusion multiple et à la réponse inadéquate des détecteurs.

CRDV R-4343/84 (NON CLASSIFIE)

Bureau - Recherche et Développement, MDN, Canada.
CRDV, C.P. 8800, Courcelette, Qué. G0A 1R0

"Méthode d'inversion de l'équation lidar" par B.T.N. Evans

On a modifié la méthode d'inversion développée par Klett pour l'équation lidar. La validité et l'exactitude de cette nouvelle méthode sont démontrées. Contrairement aux méthodes déjà connues, la modification permet d'éviter l'emploi d'une estimation pour déterminer l'extinction à chaque retour du rayonnement lidar.

On discute aussi des autres méthodes d'inversion. On souligne l'importance des hypothèses dans le développement de l'équation lidar pour la diffusion unique et la méthode d'inversion. On accorde une attention spéciale à la relation entre la rétrodiffusion et l'extinction totale, à la diffusion multiple et à la réponse inadéquate des détecteurs.

CRDV R-4343/84 (NON CLASSIFIE)

Bureau - Recherche et Développement, MDN, Canada.
CRDV, C.P. 8800, Courcelette, Qué. G0A 1R0

"Méthode d'inversion de l'équation lidar" par B.T.N. Evans

On a modifié la méthode d'inversion développée par Klett pour l'équation lidar. La validité et l'exactitude de cette nouvelle méthode sont démontrées. Contrairement aux méthodes déjà connues, la modification permet d'éviter l'emploi d'une estimation pour déterminer l'extinction à chaque retour du rayonnement lidar.

On discute aussi des autres méthodes d'inversion. On souligne l'importance des hypothèses dans le développement de l'équation lidar pour la diffusion unique et la méthode d'inversion. On accorde une attention spéciale à la relation entre la rétrodiffusion et l'extinction totale, à la diffusion multiple et à la réponse inadéquate des détecteurs.

CRDV R-4343/84 (NON CLASSIFIE)

Bureau - Recherche et Développement, MDN, Canada.
CRDV, C.P. 8800, Courcelette, Qué. G0A 1R0

"Méthode d'inversion de l'équation lidar" par B.T.N. Evans

On a modifié la méthode d'inversion développée par Klett pour l'équation lidar. La validité et l'exactitude de cette nouvelle méthode sont démontrées. Contrairement aux méthodes déjà connues, la modification permet d'éviter l'emploi d'une estimation pour déterminer l'extinction à chaque retour du rayonnement lidar.

On discute aussi des autres méthodes d'inversion. On souligne l'importance des hypothèses dans le développement de l'équation lidar pour la diffusion unique et la méthode d'inversion. On accorde une attention spéciale à la relation entre la rétrodiffusion et l'extinction totale, à la diffusion multiple et à la réponse inadéquate des détecteurs.